Graphene-MoS$_2$-Au-TiO$_2$-SiO$_2$ Hybrid SPR Biosensor: A New Window for Formalin Detection

Md. Biplob Hossain[1*], M. M. Rahman Khan[2], Md. Sadiqur Rahman[2], S. S. Bin Badrudduza[2], M. M. Sabiha[2], Md. Masud Rana[3]

1. Department. of Electrical and Electronic Engineering, Jashore University of Science and Technology, Jashore, Bangladesh
2. Department. of Electrical and Electronic Engineering, Bangladesh Army University of Engineering & Technology, Natore, Bangladesh
3. Department. of Electrical and Electronic Engineering, Rajshahi University of Engineering & Technology, Rajshahi, Bangladesh
E-mail: biplobh.eee10@gmail.com[*]

Abstract: In this article, numerically a surface plasmon resonance (SPR) biosensor is developed based on Graphene-M$_O$S$_2$-Au-TiO$_2$-SiO$_2$ hybrid structure for formalin detection. This developed sensor sensed the presence of formalin by applying attenuated total reflection (ATR). In ATR method, we developed and observed two characteristics curve, one is "SPR angle versus minimum reflectance (R_{min})" and another is "SPR frequency (SPRF) versus maximum transmittance (T_{max}). In the proposed sensor, Chitosan is used as probe legend to perform specific reaction with the formalin (40% formaldehyde) as target legend. Here, graphene and MoS$_2$ both are used as biomolecular acknowledgment element (BAE). And TiO$_2$ as well as SiO$_2$ bilayers are used to improve sensor sensitivity and Gold (Au) is to sharp SPR curve. In numerical results, the variation of SPRF and SPR angle for inappropriate sensing of formalin is quiet insignificant which confirms the absence of formalin. On the other hand, these variations for appropriate sensing is considerably significant that confirms the presence of formalin. At the end of this article, a study of variation of sensitivity of the proposed biosensor in corresponding to the increment of refractive index with a refractive index step 0.01 RIU is measured. In inclusion of TiO$_2$-SiO$_2$ bilayers with Graphene-M$_O$S$_2$, maximum sensitivity of 85.375% more is numerically reported.
Keywords: Biosensor; Surface plasmon resonance; Formalin detection; Resonance angle; Resonance frequency.

1. Introduction

Formalin (40% formaldehyde) is a toxic element soluble in water, has been classified as Group I Carcinogen to human beings by the International Agency for Research on Cancer (IRAC) [1]. Recent news and research have claimed the use of formaldehyde in food preservation that is very popular, particularly in Asian countries [1]. As a result, the detection of formalin is a concerned issue which is a biochemical process. Its mechanism of action for fixing lies in its ability to form cross-links between soluble and structural proteins. The resulting structure retains its cellular constituents in them in vivo relationships to each other, giving it a degree of mechanical strength, which enables it to withstand subsequent processing, as reported by Environmental and Occupational health and Safely Services 2004 [2].

Nowadays, Biosensors have been deeply researched owing to their importance of many industry applications such as medical diagnosis, enzyme detection, food safety and environmental monitoring [3, 4]. Today numeral biosensors have been technologically advanced, among them SPR biosensor bears the advantage of compactness, light weight, high sensitivity, the case of multiplexing and remote sensing and so forth [5]. SPR wave is a momentary guided electromagnetic wave that propagates along a metal-dielectric interface by utilizing the surface plasmon waves (SPW). The variation of the biomolecules concentration on account of chemical reaction, will produce the local modification of the surrounding refractive index (RI) near the sensor surface that outcomes in altering the propagation constant of the SPW and thus the SPR angle and SPR frequency (SPRF) changes [6]. The SPR technique has been successfully applied in various fields, such as chemical and biochemical sensing, film characterization and beam characterization.

In the present paper, a numerically Graphene-MOS$_2$-Au-TiO$_2$-SiO$_2$ hybrid coated SPR biosensor is developed for formalin detection which results in faster immobilization by monitoring the change of SPR angle-minimum reflectance attributor and SPR frequency-maximum transmittance attributor. Composite structure is used due to

graphene has high adsorption ability and optical characteristics [7-12], MoS_2 has high flurescence quenching ability [11], and TiO_2 & SiO_2 show tremendous plasmonic effect near to TiO_2-SiO_2 interface facilitating effective light trapping [11]. These effective light trapping generates more surface plasmons (SPs) which will eventually enhance the SPR angle and frequency. This rise of SPR angle and frequency will increase the SPR sensing [12]. Molecular concentration is varied due to the immobilization of probe molecule on the sensor surface that changes the refractive index (RI)) near the graphene-MoS_2 layer [10-12]. The RI change will in turn prime to change in the SPR angle and SPR frequency attributor that explains a change in propagation constant of SPW [6].

2. Methodology

A schematic of the proposed composite layered SPR biosensor is shown in Fig. 1. On the basis of kretschmann angular interrogation configuration of SPR technology, a composite layer of graphene-MoS_2-Au-TiO_2-SiO_2 is deposited on the base of prism and this whole arrangement kept in contact with the water or sample containing the target biomolecule/ chemical also known as analytes, for sensing application [12]. The sensor layers are defined as the first layer is SF11 glass prism (RI, n_p=1.7786) [12]; second layer is TiO_2 (RI, n_2=2.5837) [13], 3rd layer is SiO_2 (RI, n_3=1.4570) [12], 4th layer is Au (RI, n_4= 0.1838+i*3.4313) [14], 5th layer is MoS_2 (RI, n_5=5.9+i*0.8) [12], 6th layer is graphene (RI, n_6=3.0 + i 1.1487) [12] and final layer is water (RI n_7=1.33) [6]. After settling the setup, a TM polarized He-Ne (wavelength = 633 nm) light wave is used, which passes through the prism and some portion is reflected at the prism-gold interface. During intruding light energy to prism-gold interface, an evanescent wave is generated which is known as surface plasmon wave (SPW) mentioning in *Introduction* section that propagates with the different propagation constant from optical wave which is defined in Eq. 4. The propagation constant of SPW can be adjusted to be equal to the propagation constant of optical wave. The point at which optical wave propagation constant equals SPW propagation constant is called SPR point [6]. In Eq. 1, it depicts that SPR angle is a dependent parameter on RI of sensing medium. At SPR point, the frequency at which SPW propagates is called surface resonance frequency (SRF) and the angle of incidence is called SPR angle that can be given as follows:

$$\theta_{SPR} = a \sin \sqrt{\frac{(n^2{}_{com}n^2{}_s)}{n^2{}_p(n^2{}_{com}+n^2{}_s)}} \tag{1}$$

The reflectance spectra show a dip at the resonance condition when the wave vector of the incident light matches with the SPW. Here, n_{com} refers equivalent RI of *Graphene-M_OS_2-Au-TiO_2-SiO_2* composite layer which is defined as:

$$\theta_{com} = \sqrt[5]{n_2 n_3 n_4 n_5 n_6} \tag{2}$$

When formalin is flowing through chitosan on the sensor surface according to the Fig. 2, then the RI of sensing medium is modified owing to performing chemical reaction as follows [6]:
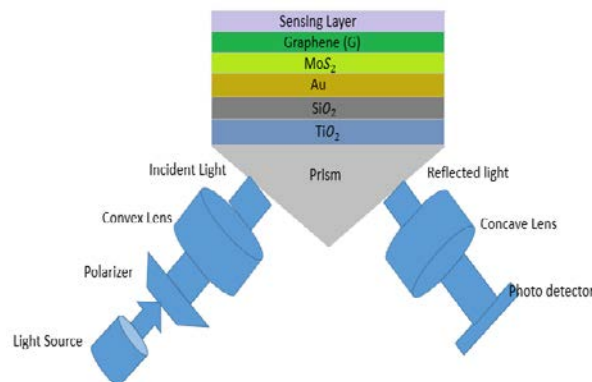
Fig 1. Schematic of *graphene-M_OS_2-Au-TiO_2-SiO_2* modeled ultrasensitive hybrid layer biosensor for formalin detection.

$$n_s^2 = n_s^1 + c_a \frac{dn}{dc} \tag{3}$$

Here, n^2_s is the RI of the sensing dielectric after adsorption of formaldehyde molecules, n^1_s is the RI of the sensing dielectric before adsorption of formaldehyde molecules, C_a is the concentration of adsorbed bio molecules, and *dn/dc* is the RI increment. For water the increment factor is 0.181 cm³/gm [15]. If SPR angle changes, the propagation constant of SPW also changes which has been explained mathematically in the literature [5] as given below:

$$K_{SPW} = \frac{2\Pi}{\lambda} n_p \, sin \, \theta_{SPR} \tag{4}$$

The majority of SPR applications connect with the real RI changes due to chemical or biochemical action [1] and therefore, Eq. 1 is formed by considering real quantities only. A resonant excitation of photon-electron coupling takes place when the wave vector of the incident light matches that of the SPW (Surface plasmon wave), these two are equal, which produces shift of incident angle. The total reflectance vs angle of incidence or reflectance vs wavelength characteristics curve is known as the SPR curve. Finally, if propagation constant of SPW changes it makes the surface resonance frequency (SRF) change which can be explained by the following equation [16,17]:

$$SPRF = \frac{C_o}{n_{com}} \frac{K_{SPW}}{2\Pi} \tag{5}$$

Where C_0/n_{com} is the propagation velocity of SPW that is a perpendicularly confined evanescent electromagnetic wave [17-20].
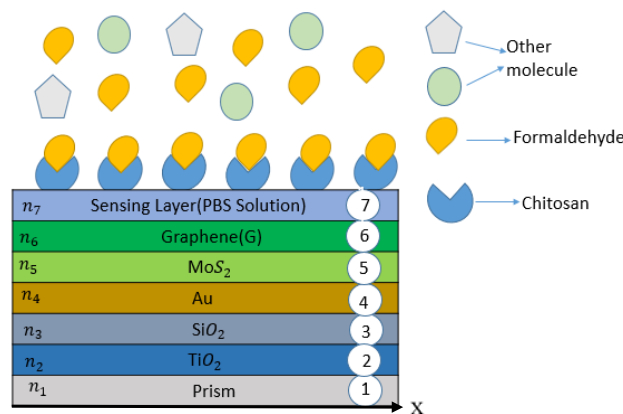
Fig 2. Formaldehyde Detection through Immobilization of Bio Agents Using Chitosan.

If the incident angle of optical wave is tuned, SPR condition is achieved in which reflectance (R) of reflected wave is minimum and transmittance (T) is maximum and then then SPW penetrate at SPF along the x-direction. We define two plot "transmittance versus surface resonance frequency (T~SRF curve)," as well as "Reflectance versus surface resonance angle (R~SPR-angle curve)," as surface resonance attributor. To make a SPFR curve, we used Fresnel equation for five-layered heteroptical system to determine reflected light intensity [6]. The reflected power for TM-polarized light is as [6]:

$$R = \frac{A + \frac{B}{Z_f} - z_i(C + \frac{D}{Z_f})}{A + \frac{B}{Z_f} + z_i(C + \frac{D}{Z_f})} \tag{6}$$

Here, Z_i and Z_f are initial and final layer wave impedances respectively in the structure of Fig 1. An individual layer wave impedance can be determined using as [6]:

$$Z_f = \frac{K_s(n_k \, cos \, \theta)}{\omega \varepsilon_k^2} \tag{7}$$

In Eq.7, n_k and ϵ_k are refractive index (RI) and permittivity of kth layer, $\omega = 2\pi c/\lambda$ and k_s is the light wave vector. The variables A, B, C and D in Eq. 6 that can be calculated by solving the following matrix equation as [6]:

$$\begin{bmatrix} A & B \\ C & D \end{bmatrix} = \begin{bmatrix} A_2 & B_2 \\ C_2 & D_2 \end{bmatrix} \times \begin{bmatrix} A_3 & B_3 \\ C_3 & D_3 \end{bmatrix} \times \ldots\ldots \times \begin{bmatrix} A_{N-1} & B_{N-1} \\ C_{N-1} & D_{N-1} \end{bmatrix} \tag{8}$$

Eq. 8, represents generalized interfacial layer system. Here, first layer represents reflectance, therefore they are not present in the matrix equation. In matrix, each element describes the reflection terms of an individual layer. These are the subscripted variables A, B, C and D of each matrix and can be found by the following equation set [6]:

$$\begin{cases} A_k = \cos(d_k \omega \varepsilon_k^2 \cos\theta_k) \\ B_k = z_k \cos(d_k \omega \varepsilon_k^2 \cos\theta_k) \\ B_k = \dfrac{\sin(d_k \omega \varepsilon_k^2 \cos\theta_k)}{z_k} \\ D_k = \cos(d_k \omega \varepsilon_k^2 \cos\theta_k) \end{cases} \tag{9}$$

Here, d_k, θ_k and Z_k are the thickness, angle of incidence and wave impedance of kth layer respectively. The angle of incidence of kth layer is unknown that can be found as a function of the refractive index of the initial and k^{th} layer as [6]:

$$\theta_k = cos^{-1}\left(\sqrt{1 - \frac{n_k}{n_{k+1}} sin^2\theta} \right) \tag{10}$$

Light with a wavelength of 633 nm is emitted from a monochromatic source, and the corresponding data are collected with a spectrometer and computer.

3. Numerical results analysis

Numerical analysis is initiated by checking the R~SPR-angle curve and T~SPRF curve in the absence of formalin (target ligand) and chitosan (probe ligand) which is normally known as bare sensor, as shown in Fig. 3. In our SPR device, water is used as sensing medium that helps to measure the dependency of reflectance on SPR angle and transmittance on SPRF. The work is continued by assuming that our sensor is susceptible of differentiating between probe element (chitosan) and detectionable target with regard to the analysis of detection or not. It is necessary to increase the SPR angle and SPR frequency in the right side of the R~SPR angle and T~SRF curve due to using Nano film TiO_2-SiO_2 layer whose phenomenon accounts for enhanced sensitivity [12].
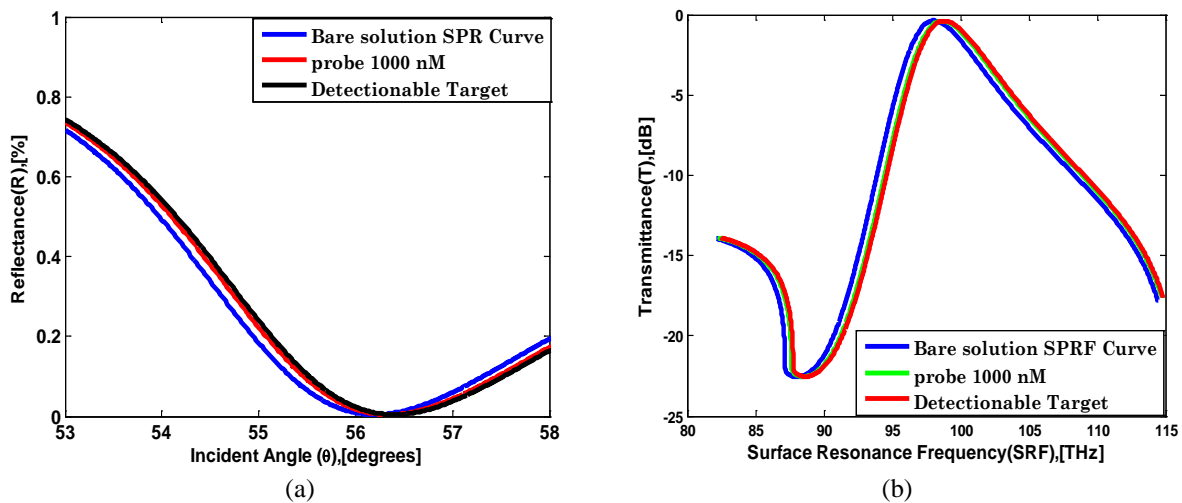
Fig 3. Characteristics curve of bare SPR Sensor (a) R~SPR-angle curve in the absence of formalin and presence of chitosan. (b) T~SRF curve in the absence of formalin and presence of chitosan.

Fig. 3(a) and 3(b) are demonstrating R~SPR-angle and T~SPRF curve. The blue line (—) in Fig. 3(a) and 3(b), show the SPR angle (56.26^0) and SPRF (97.968 THz) during both probe (chitosan) and target (formalin) are absent respectively. The angle of incidence and SPRF of bare sensor are 56.26^0 and 97.968 THz respectively. The green line (—) shows the SPR angle (56.34^0) and SPRF (98.688) while 1000 nM probe (chitosan) are placed to water

respectively. The change of detecting attributor ($\Delta\theta_{SPR}$ & R_{min}) and (ΔSPRF & T_{max}) due to adding formalin is provided in Table 1. The information of Table 1 has been extracted from Fig. 4(a) and 4(b).
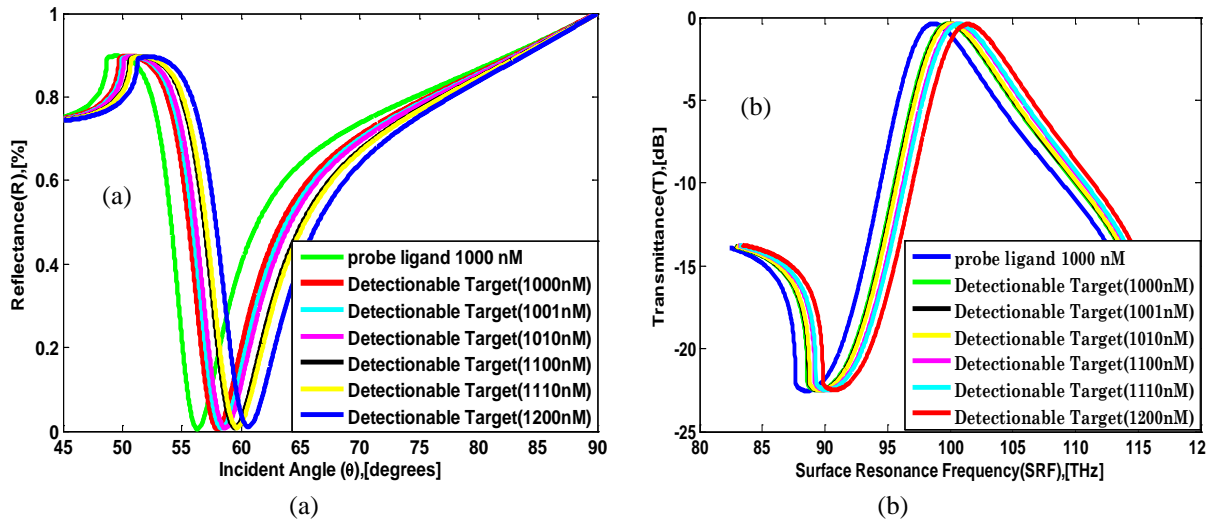
Fig 4. (a) Reflectance vs. Incident Angle Curve and (b) Transmittance vs. SPR Frequency Curve for Different Concentration of Detectionable Target.

Table 1. R_{min}[%], θ_{SP} [deg], T_{max} [dB] and SPRF [THz] for different concentrated dielectric medium (formalin, ranging 1000nM to 1200 nM)

Concentration (C_a)	R_{min} [%]	θ_{SP} [deg]	T_{max} [dB]	SPRF [THz]
1000 nM Probe	0.0044	56.3400	0.3795	98.688
1000 nM Target	0.0062	58.0500	0.3981	99.875
1001 nM Target	0.0066	58.3800	0.4002	100.008
1010 nM Target	0.0070	58.6700	0.4018	100.106
1100 nM Target	0.0082	59.4900	0.4106	100.627
1110 nM Target	0.0085	59.6800	0.4129	100.761
1200 nM Target	0.0100	60.6200	0.4249	101.447

Since the change of concentration is due to immobilization of chitosan within the sensing medium, the local RI of the sensing medium is also changed followed by Eq. 2. In Eq. 1, it is stated that SPR angle changes if n_s changes which finally translates k_{spw} change that observed from Eq. 3. At the transition point where the SPW wave vector and optic wave vector are equal to each other, the minimum reflectance (R_{min}) and maximum transmittance (T_{max}) are detected. As illustrated in Fig. 3, before reaction of formalin with probe ligand added on the sensor device, no significant change in SPR angle ($\Delta\theta_{res}$=0.06) and in frequency (ΔSPRF=0.15) are occurred due to its no bonding reaction between probe ligand and sensing target.

Upon making a bond with the target, the chemical bonding configuration changes, which leads to the change in the optical properties. Hence it would be observed whether there is formalin in the sample or not. Also increased amount of formalin forms more recurring bonds thus indicating greater interaction [19], [20]. The amount of shift rises with the increasing concentration of the detectionable target from 1 to 200 nM as stated by analytical data in Table 1 for reflectance and transmittance. The amount of these changes would determine whether the formalin detection event would occur in the presence of binding formalin or not.

In detection approach, firstly, we find out the values of $(\Delta R_{min}^{P-T})_{min}$ & $(\Delta\theta_{SPR}^{P-T})_{min}$ and $(\Delta SPRF_{p-t})_{min}$ & $(\Delta T_{max}^{p-t})_{min}$ from table 1 by using the following Eq. set (5). And setting these values as threshold parameters.

$$\begin{bmatrix} (\Delta R_{min}^{P-T})_{min} = \left|R_{min}^{Probe} \sim R_{min}^{Target}\right| = |0.0044 \sim 0.0062| = 0.0018 \cdots\cdots\cdots\cdots\cdots (a) \\ (\Delta\theta_{SPR}^{P-T})_{min} = \left|\theta_{SPR}^{Probe} \sim \theta_{SPR}^{Target}\right| = |56.340 \sim 58.050| = 1.71 \cdots\cdots\cdots\cdots\cdots\cdots (b) \\ (\Delta T_{max}^{P-T})_{min} = \left|T_{max}^{Probe} \sim T_{max}^{Target}\right| = |0.3795 \sim 0.3981| = 0.0186 \cdots\cdots\cdots\cdots\cdots (c) \\ (\Delta SPRF^{P-T})_{min} = \left|SPRF^{Probe} \sim SPRF^{Target}\right| = |98.688 \sim 99.875| = 1.187 \cdots (d) \end{bmatrix} \quad (11)$$

Here, R_{min}^{Probe} represents the minimum reflectance of probe ligand (chitosan), R_{min}^{Target} denotes the minimum reflectance of sampling target, θ_{spR}^{Probe} depicts the SPR angle of probe ligand and finally θ_{spR}^{Target} is the SPR angle

of sampling target. We reached the same conclusion by taking ΔSRF_{p-t} and ΔT_{max}^{p-t} also as the detecting attributors. Then we determined the change of minimum reflectance, change of SPR angle, change of maximum transmittance and change of SPRF for different concentrated formalin molecules by using the data in Table 1 and tabulated to table 2.

Table 2. Calculated ΔR_{min}^{P-T} [%], ΔT_{max}^{p-t} , ΔSRF_{p-t} [THz] and $\Delta \theta_{sp}^{P-T}$ [deg] values from Equ. 5 for different concentration of dielectric medium.

Concentration (C$_a$) (nM)	$\Delta R_{min}^{P-T}(\%)=$ $\lvert R_{min}^{Probe} - R_{min}^{Target} \rvert$	$\Delta \theta_{spR}^{P-T}(deg)=$ $\lvert \theta_{spR}^{Probe} - \theta_{spR}^{Target} \rvert$	$\Delta T_{max}^{p-t} (dB)=$ $\lvert T_{max}^{Probe} - T_{max}^{Target} \rvert$	$\Delta SPRF_{p-t} (THz)=$ $\lvert SPRF_{probe} - SPRF_{Target} \rvert$
1000 (Target)	$(\Delta R_{min}^{P-T})_{min}$	$(\Delta \theta_{spR}^{P-T})_{min}$	$(\Delta T_{max}^{p-t})_{min}$	$(\Delta SRF_{p-t})_{min}$
1001 (Target)	0.0022	2.04	0.0207	1.32
1010 (Target)	0.0026	2.33	0.0223	1.418
1100 (Target)	0.0038	3.15	0.0311	1.939
1110 (Target)	0.0041	3.34	0.0334	2.073
1200 (Target)	0.0056	4.28	0.0354	2.759

The numerical data appraises the strong dependency of the SPR angle and SPRF on the concentration increment that reflects in reflectance and transmittance characteristics curve.

If the measured values are greater than these threshold parameters, then we observed the presence of formalin in that target sample. For clarifying detection condition we obtained a decision and tabulated in table 3. These values can really give an idea about successful interaction or the failed ones. The first condition in table 3 expresses the desired condition, second and third one needs careful recheck for attaining desired condition, fourth condition confirms the probe is still free and without a target molecule.

Table 3. Four Probable Conditions for Making Decision about Successful Interaction.

Conditions for using & R$_{min}$ as detecting attributor	Conditions for using ΔSPRF & T$_{max}$ as detecting attributor	Decision
$\Delta R_{min}^{P-T} \geq (\Delta R_{min}^{P-T})_{min}$ && $\Delta \theta_{spR}^{P-T} \geq (\Delta \theta_{spR}^{P-T})_{min}$	$\Delta T_{max}^{p-t} \geq (\Delta T_{max}^{p-t})_{min}$ && $\Delta SPRF_{p-t} \geq (\Delta SPRF_{p-t})_{min}$	Formalin is detected
$\Delta R_{min}^{P-T} \geq (\Delta R_{min}^{P-T})_{min}$ && $\Delta \theta_{spR}^{P-T} \leq (\Delta \theta_{spR}^{P-T})_{min}$	$\Delta T_{max}^{p-t} \geq (\Delta T_{max}^{p-t})_{min}$ && $\Delta SPRF_{p-t} \leq (\Delta SPRF_{p-t})_{min}$	Re-evaluate
$\Delta R_{min}^{P-T} \leq (\Delta R_{min}^{P-T})_{min}$ && $\Delta \theta_{spR}^{P-T} \geq (\Delta \theta_{spR}^{P-T})_{min}$	$\Delta T_{max}^{p-t} \leq (\Delta T_{max}^{p-t})_{min}$ && $\Delta SPRF_{p-t} \geq (\Delta SPRF_{p-t})_{min}$	Re-evaluate
$\Delta R_{min}^{P-T} \leq (\Delta R_{min}^{P-T})_{min}$ && $\Delta \theta_{spR}^{P-T} \leq (\Delta \theta_{spR}^{P-T})_{min}$	$\Delta T_{max}^{p-t} \leq (\Delta T_{max}^{p-t})_{min}$ && $\Delta SPRF_{p-t} \leq (\Delta SPRF_{p-t})_{min}$	Free Probe

The SPR angle shifts rightward in SPR curve with the increment of refractive index followed by Eq. 1. Here, shifting of SPR angle with the increment of refractive index having step size δC_n= 0.01 is measured and the corresponding increment of sensitivity of the proposed biosensor according to the Eq. 8, in literature [8], is also determined and graphically shown in Fig. 5. From Fig. 5, it is observed that the sensitivity for without TiO$_2$, SiO$_2$, MoS$_2$ and Graphene (conventional structure) is very poor ranging 70.44% to 75.26% with respect to the sensing medium RI (ranging n_s=1.34 to n_S=1.41 respectively). After then the sensitivity for without TiO$_2$, SiO$_2$ and MoS$_2$ but with graphene ranges from 71.62% to 76.24%, which is comparatively better than the conventional structure. Further, the sensitivity without TiO$_2$, SiO$_2$ and graphene but with MoS$_2$ covers 76.44% to 81.82%. After that, if both graphene and MoS$_2$ are used and TiO$_2$ and SiO$_2$ are not used then sensitivity improves than the previous structures which covers 77% to 82.40%. Now, if SiO$_2$ layer is used with the Graphene-MoS$_2$ and TiO$_2$ is not used then the sensitivity enhances ranging 78% to 85.14%.

More again, if TiO$_2$ layer is used instead of SiO$_2$ layer in the previous structure, then just like before the sensitivity keeps almost constant. If we used all the layers at a time, which is proposed in this work, then the sensitivity is the highest among all the previous structures, which covers the range from 79% to 85.375%. We compare the main performance parameter i.e. sensitivity with different sensor structure for 1.41 RIU refractive index and tabulated these data in table 4.
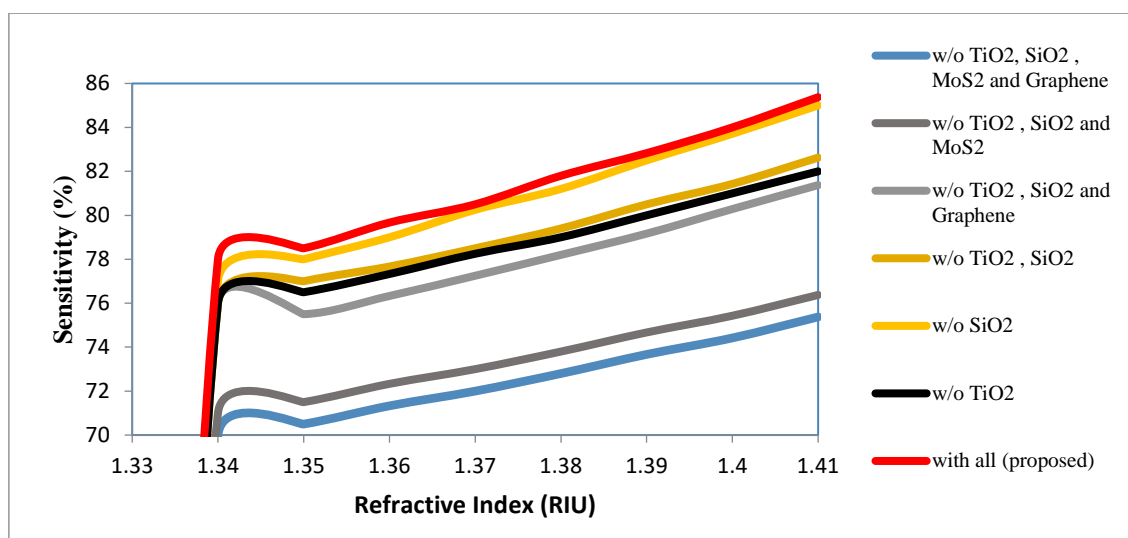
Fig. 5. Percentage of sensitivity vs. Refractive Index curve for different proposed structure.

Table 4. Analysis of sensitivity corresponding to sensing layer refractive index of 1.41 for seven different structures at the optimum thickness of TiO_2, SiO_2 and monolayer of MoS_2 and graphene.

Modeling structure	Sensitivity (s) [%RIU^{-1}] (n_S=1.41)
Without TiO2, SiO2, MoS2 and Graphene	75.26
Without TiO2, SiO2 and MoS2 and with graphene	76.24
Without TiO2, SiO2 & graphene and with MoS_2	81.82
With graphene & MoS2 and without TiO2 & SiO2	82.40
With graphene, SiO2 & MoS2 and without TiO2	85.14
With graphene, TiO2 & MoS2 and without SiO2	82.10
With Graphene-MoS2-TiO2-SiO2 (Proposed)	85.375

4. Conclusions

In this article, a numerical analysis is investigated to notice the consequence of adding of graphene, MoS_2, TiO_2 and SiO_2 layer step by step on sensitivity parameters for formalin detection. The first concern of this study is to detect the presence the formalin based ATR method by noting the change of "SPR angle versus minimum reflectance" attributor and "SPRF versus maximum transmittance" attributor. Here, chitosan, we used as probe legend to react with formalin (formaldehyde). The second concern is sensitivity analysis by adding of graphene, MoS_2, TiO_2 and SiO_2 layer step by step. Graphene as well as MoS_2 thin films play important roles to develop electro-optical sensor device due to their biocompatibility, high surface to volume ratio, low isoelectric point and better chemical stability properties make it very suitable for such kind of application like formalin detection. For plasmonic effect near TiO_2 - SiO_2 interface the light trapping is effectively enhanced because of enhanced light trapping more surface plasmons are generated which will eventually enhance the resonance angle, this concept can indeed fulfill the maximum sensitivity requirement. Numerically 85.375% sensitivity for RI 1.41 RIU has been reported for our proposed sensor.

5. References

[1] Noor Aini B, Siddiquee S, Ampon K. Development of formaldehyde biosensor for determination of formalin in fish samples; Malabar red snapper (Lutjanus malabaricus) and longtail tuna (Thunnus tonggol). Biosensors. 2016;6(3):32.
[2] Occupational Health and Safety Amendment Regulations 2014. Victorian Work Cover Authority (VWA), June 2014. http://www.legislation.vic.gov.au/. [accessed 13 September 2014].
[3] Pumera M. Graphene in biosensing. Materials Today. 2011;14(7-8):308-315.
[4] Homola J. Present and future of surface plasmon resonance biosensors. Analytical and Bioanalytical Chemistry. 2003;377(3):528-539.

[5]   Fu H, Zhang S, Chen H, Weng J. Graphene enhances the sensitivity of fiber-optic surface plasmon resonance biosensor. IEEE Sensors Journal. 2015;15(10):5478-5482.

[6]   Hossain M, Rana M. DNA hybridization detection based on resonance frequency readout in graphene on Au SPR biosensor. Journal of Sensors. 2016;2016.

[7]   Shushama KN, Rana MM, Inum R, Hossain MB. Graphene coated fiber optic surface plasmon resonance biosensor for the DNA hybridization detection: Simulation analysis. Optics Communications. 2017;383:186-190.

[8]   Rahman MS, Anower MS, Hasan MR, Hossain MB, Haque MI. Design and numerical analysis of highly sensitive Au-MoS2-graphene based hybrid surface plasmon resonance biosensor. Optics Communications. 2017;396:36-43.

[9]   Shushama KN, Rana MM, Inum R, Hossain MB. Sensitivity enhancement of graphene coated surface plasmon resonance biosensor. Optical and Quantum Electronics. 2017;49(11):381.

[10] Rahman MS, Hossain MB, Rana MM. Sensitivity enhancement of porous silicon based SPR sensor using graphene-M0S2 hybrid structure. In: 2016 2nd International Conference on Electrical, Computer & Telecommunication Engineering (ICECTE). IEEE;2016.p.1-4.

[11] Rahman MS, Anower MS, Rahman MK, Hasan MR, Hossain MB, Haque MI. Modeling of a highly sensitive MoS2-Graphene hybrid based fiber optic SPR biosensor for sensing DNA hybridization. Optik- International Journal for Light and Electron Optics. 2017;140:989-997.

[12] Maurya JB, Prajapati YK, Singh V, Saini JP. Sensitivity enhancement of surface plasmon resonance sensor based on graphene–MoS 2 hybrid structure with TiO2–SiO2 composite layer. Applied Physics A. 2015;121(2):525-533.

[13] Jorgenson RC, Yee SS. A fiber-optic chemical sensor based on surface plasmon resonance. Sensors and Actuators B: Chemical. 1993;12(3):213-220.

[14] Maurya JB, Prajapati YK, Tripathi R. Effect of molybdenum disulfide layer on surface plasmon resonance biosensor for the detection of bacteria. Silicon. 2018;10(2):245-256.

[15] Theisen A, Johann C, Deacon MP, Harding SE. Refractive increment data-book for polymer and biomolecular scientists. Nottingham University Press; 2000.

[16] Hossain M, Rana M. Graphene coated high sensitive surface plasmon resonance biosensor for sensing DNA hybridization. Sensor Letters. 2016;14(2):145-152.

[17] Hossain MB, Hassan M, Abdulrazak LF, Rana MM, Islam MM, Rahman MS. Graphene-MoS2-Au-TiO2-SiO2 hybrid SPR biosensor for formalin detection: numerical analysis and development. Advanced Materials Letters. 2019;10(in press).

[18] Islam MM, Islam MM, Shimul YC, Rahman A, Ruhe AA, Hassan M, Hossain MB. FDTD analysis fiber optic SPR biosensor for DNA hybridization: A numerical demonstration with graphene. Journal of Materials and Applications. 2019;8(1):13-19.

[19] Hossain MB, Akib TB, Abdulrazak LF, Rana MM. Numerical modeling of graphene-coated fiber optic surface plasmon resonance biosensor for BRCA1 and BRCA2 genetic breast cancer detection. Optical Engineering. 2019;58(3):037104.

[20] Hossain MB, Rana MM, Abdulrazak LF, Mitra S, Rahman M. Graphene-MoS2 with TiO2SiO2 layers based surface plasmon resonance biosensor: Numerical development for formalin detection. Biochemistry and Biophysics Reports. 2019;18:100639.